Electronic Supplementary Information (ESI)

Enhanced Through-Plane Thermal Conductivity of Polymer Nanocomposites by Constructing Graphene-Supported BN Nanotubes

Xu Li,[a] Ya Li,[a] Md Mofasserul Alam,[b] Jibin Miao,[a] Peng Chen,[a] Ru Xia,[a] Bin Wu, *[a] and Jiasheng Qian *[a]

[a] Key Laboratory of Environment-Friendly Polymeric Materials of Anhui Province, School of Chemistry & Chemical Engineering, Anhui University, Hefei, 230601, China
[b] CAS Key Laboratory of Soft Matter Chemistry, Collaborative Innovation Centre of Chemistry for Energy Materials, School of Chemistry and Materials Science, University of Science and Technology of China, Hefei, 230026, China

Contents:

Fig. S17 the PDOS of BNNT (a) and graphene (b) in the E-G-BNNT were compared with those of pure graphene and BNNT.

Table. S1 the atomic concentration of B and N of E-G and E-G-BNNT by the XPS full spectrums.

Table. S2 the mechanical properties of the (E-G-BNNT)x/PVDF by tensile testing.

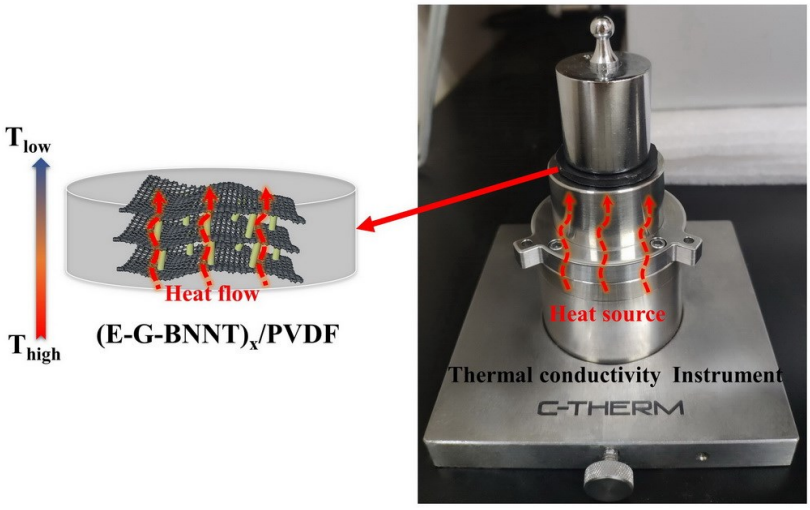

Fig. S1 the through-plane thermal conductivity of sample was measurement by TCi.

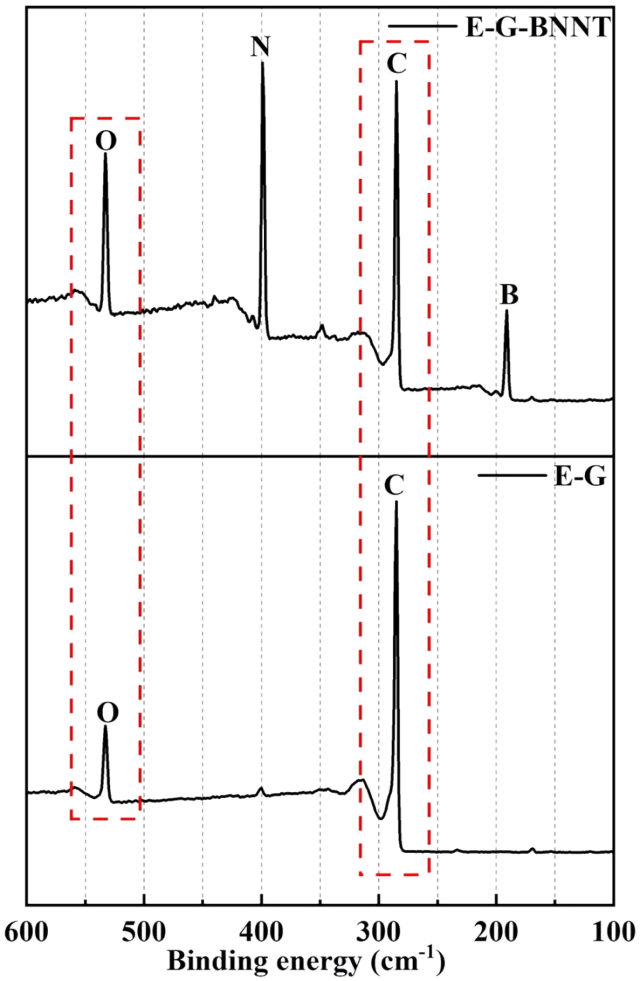

Fig. S2 the full XPS spectrums of E-G-BNNT and E-G.

Table. S1 the atomic concentration of B and N of E-G and E-G-BNNT by the XPS full spectrums.

Element	E-G (Atomic%)	E-G-BNNT (Atomic%)
B 1s	0.37	23.02
N 1s	2.02	31.01

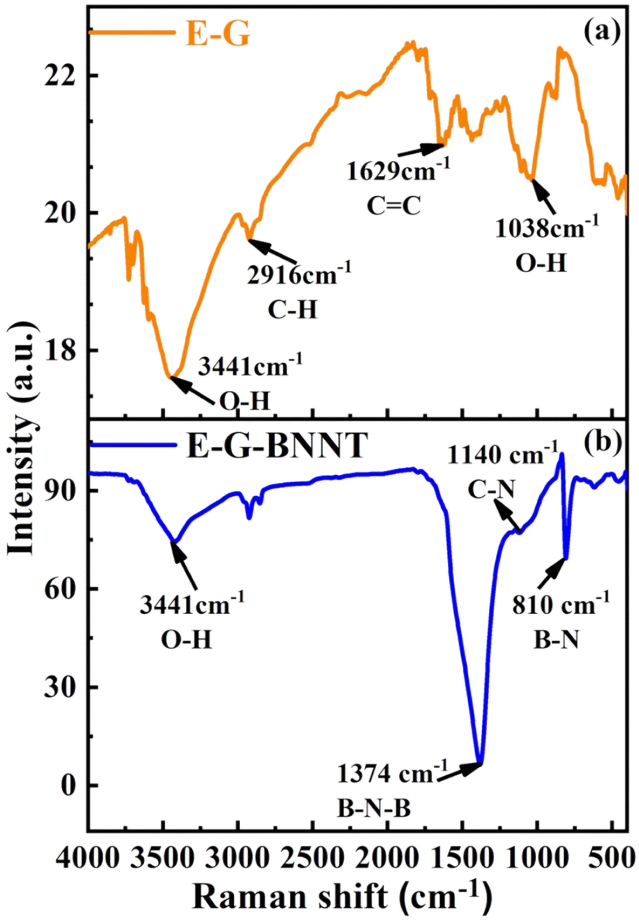

Fig. S3 the FT-IR of E-G (a) and E-G-BNNT (b)

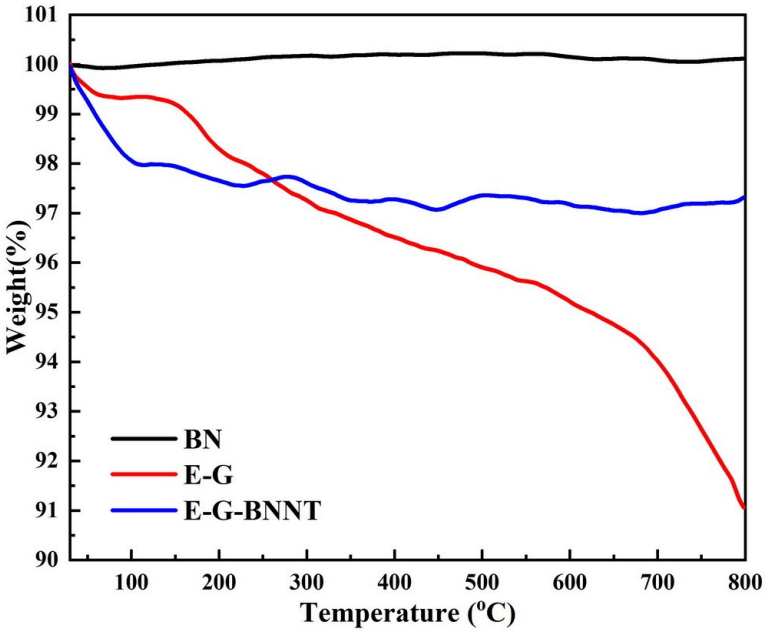

Fig. S4 the TGA of BNNS, E-G and E-G-BNNT.

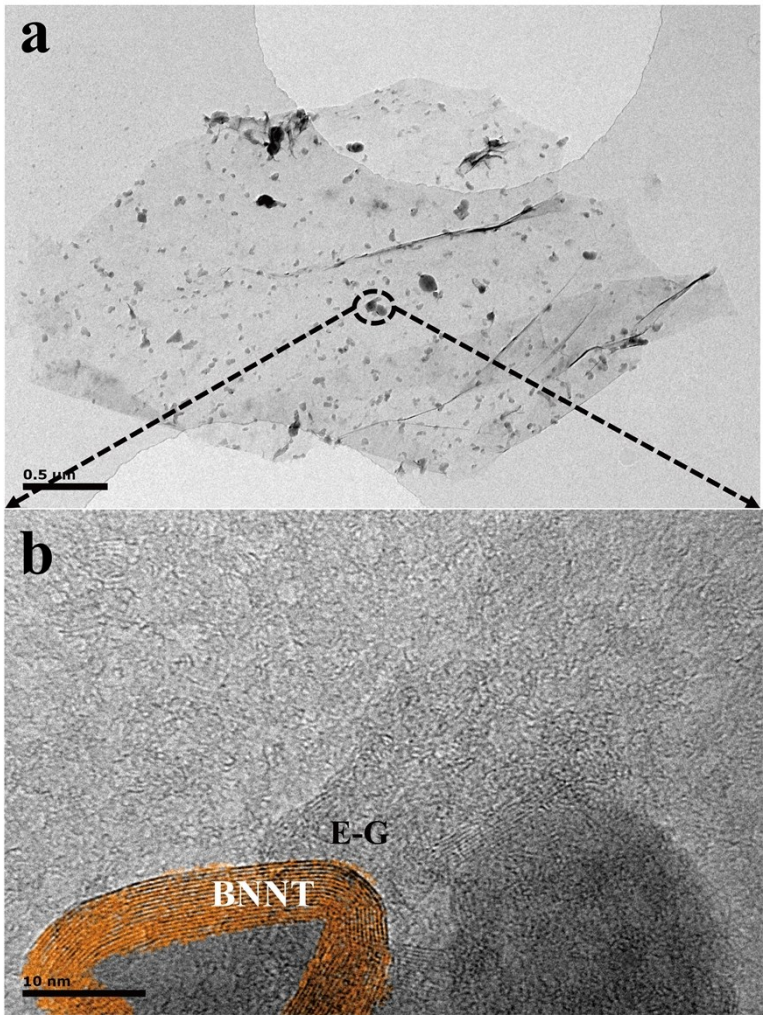

Fig.S5 TEM and HRTEM images of E-G-BNNT.

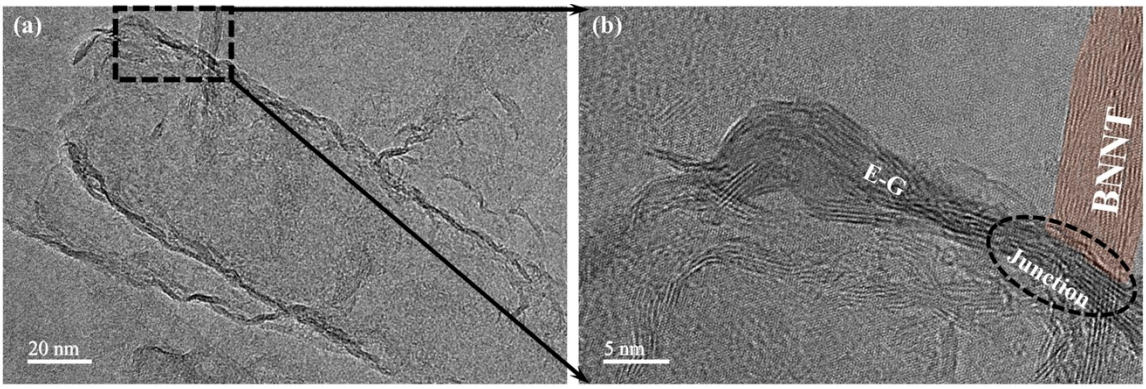

Fig. S6 the TEM of E-G-BNNT (a) and HRTEM of the junction of E-G-BNNT (b).

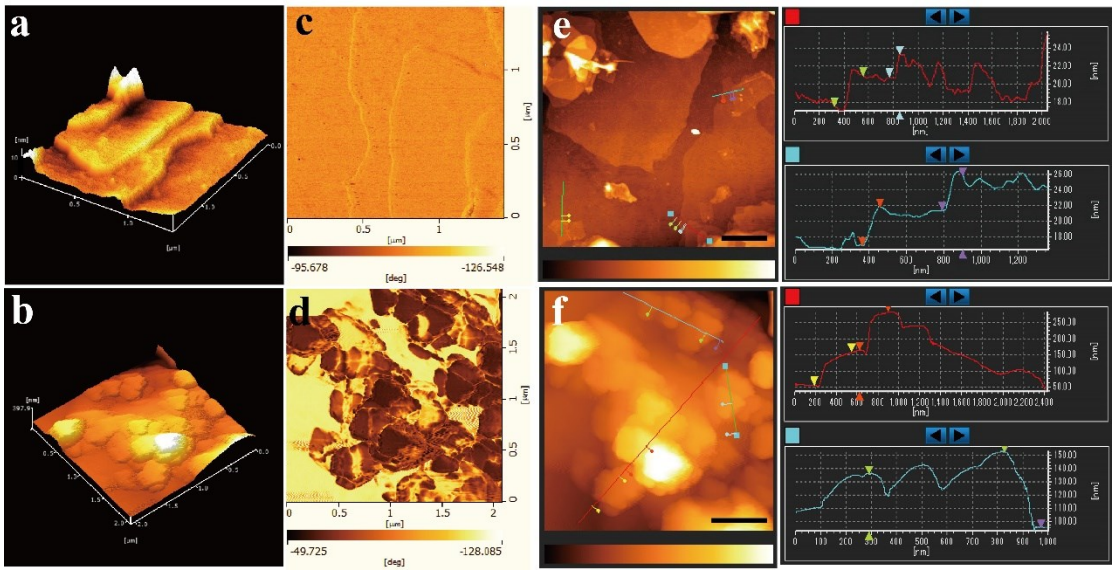

Fig. S7 the AFM of E-G (a, c, e) and E-G-BNNT (b, d, f).

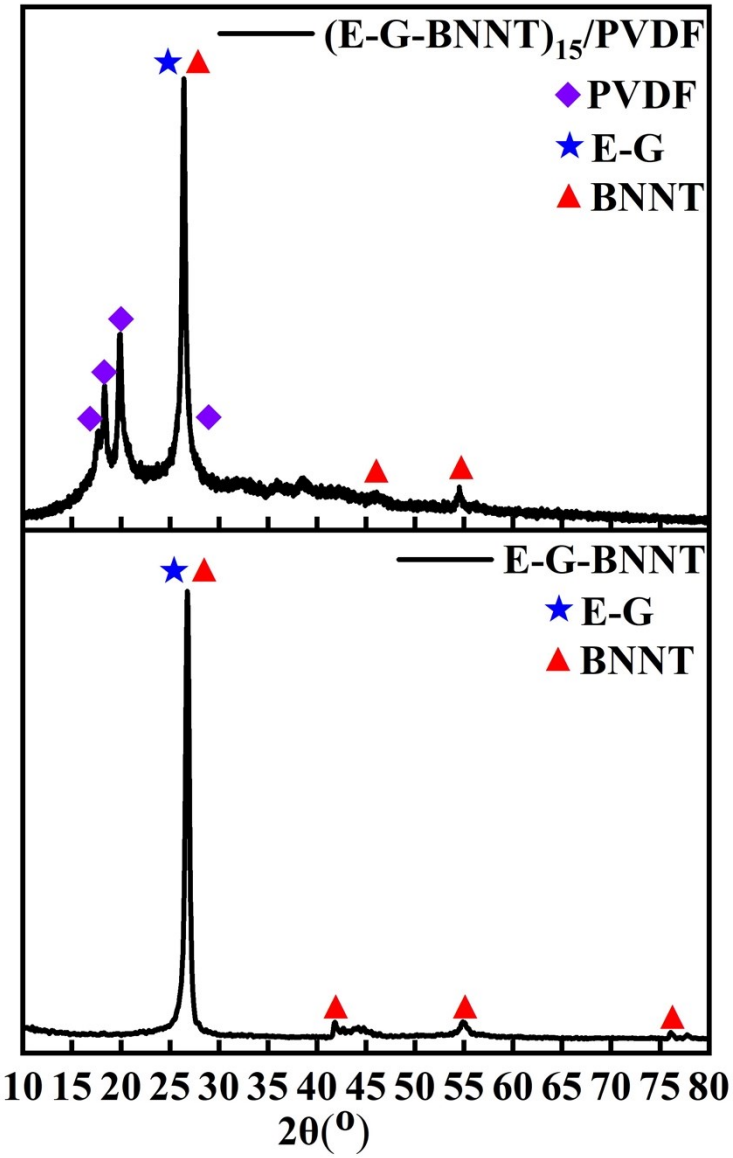

Fig.S8 the XRD of $(E\text{-}G\text{-}BNNT)_{15}$/PVDF and E-G-BNNT.

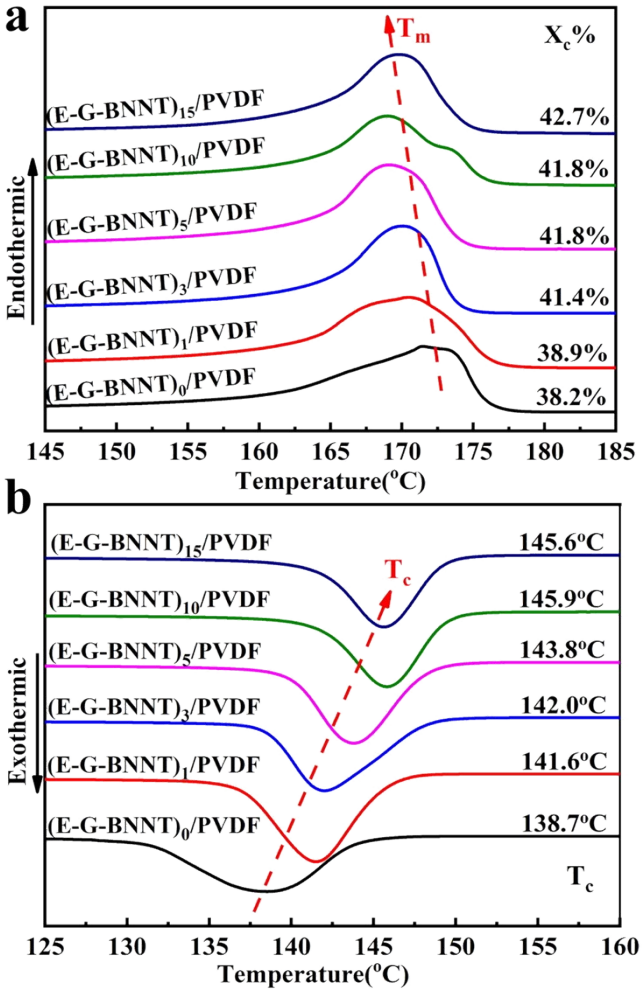

Fig. S9 the DSC heating curves (a) and cooling curves (b) of $(E\text{-}G\text{-}BNNT)_x$/PVDF with different filler loading.

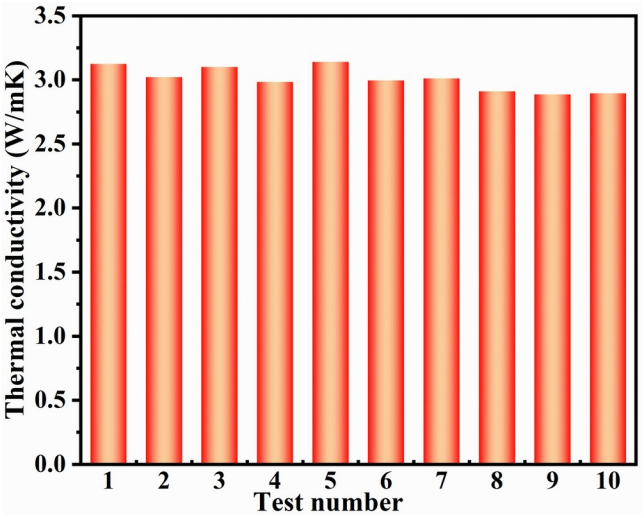

Fig. S10 the thermal conductivity of (E-G-BNNT)15-PVDF undergo 10 tests.

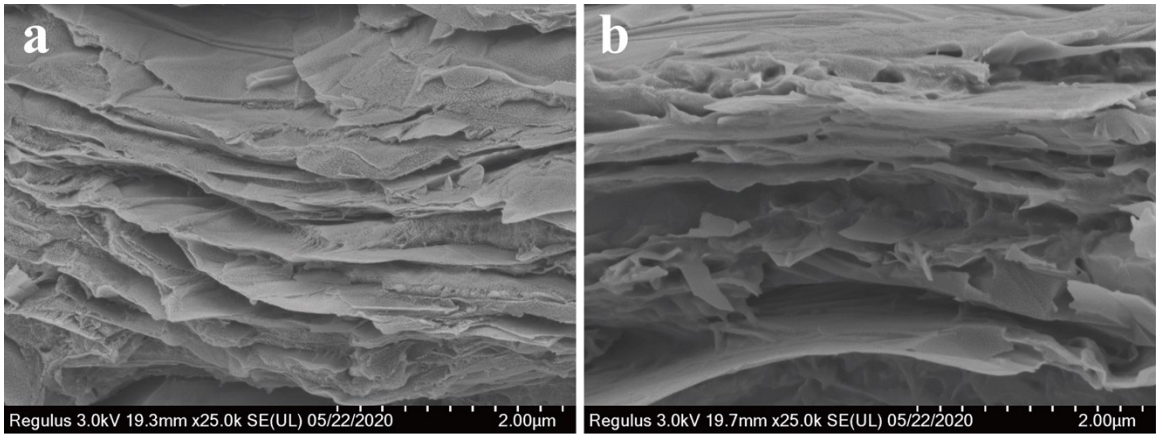

Fig. S11 the SEM of cross-section of (E-G-BNNT)$_{15}$-PVDF undergo 10 tests.

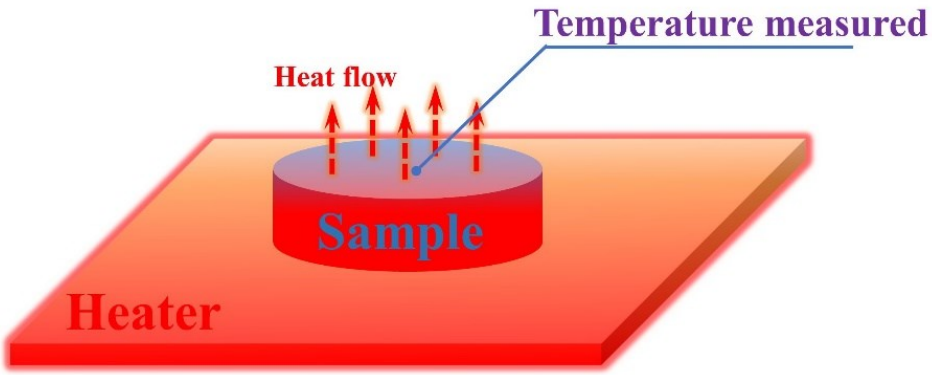

Fig. S12 the test system configuration for determining the through-plane heat-transfer capacity.

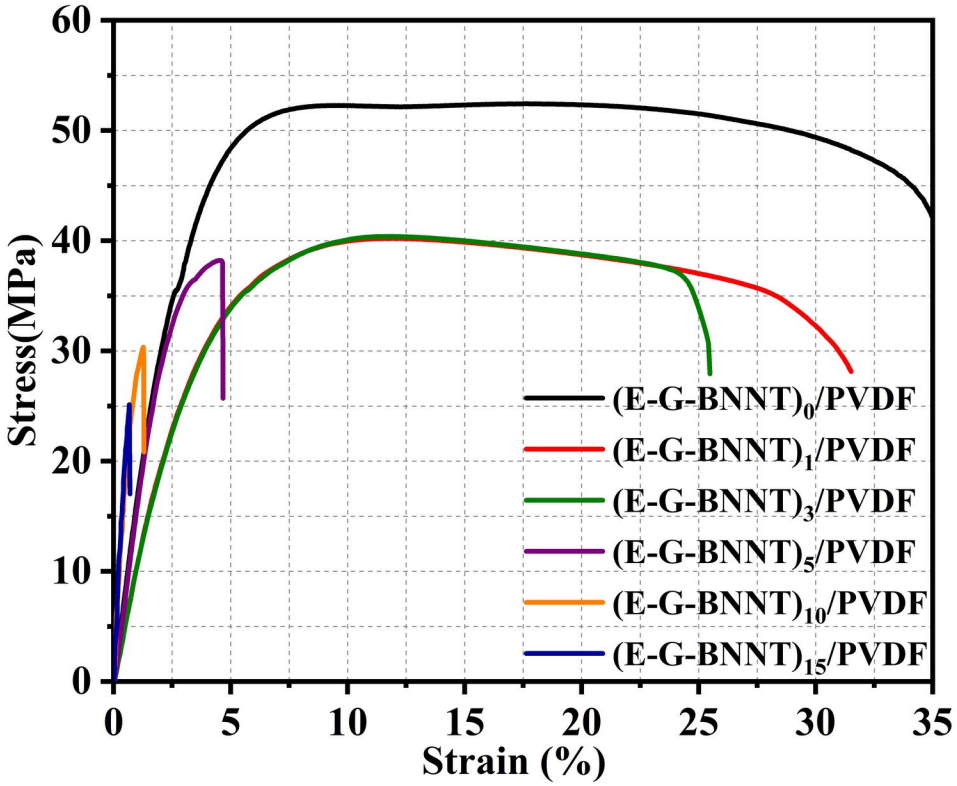

Fig. S13 the mechanical properties of the (E-G-BNNT)$_x$/PVDF with different filler loading.

Table. S2 the mechanical properties of the (E-G-BNNT)$_x$/PVDF by tensile testing.

Sample	Tensile strength (MPa)	Young's modulus (GPa)
(E-G-BNNT)$_0$/PVDF	52.43	1.73
(E-G-BNNT)$_1$/PVDF	40.21	1.09
(E-G-BNNT)$_3$/PVDF	40.39	1.10
(E-G-BNNT)$_5$/PVDF	38.21	1.67
(E-G-BNNT)$_{10}$/PVDF	30.34	7.14
(E-G-BNNT)$_{15}$/PVDF	25.12	6.28

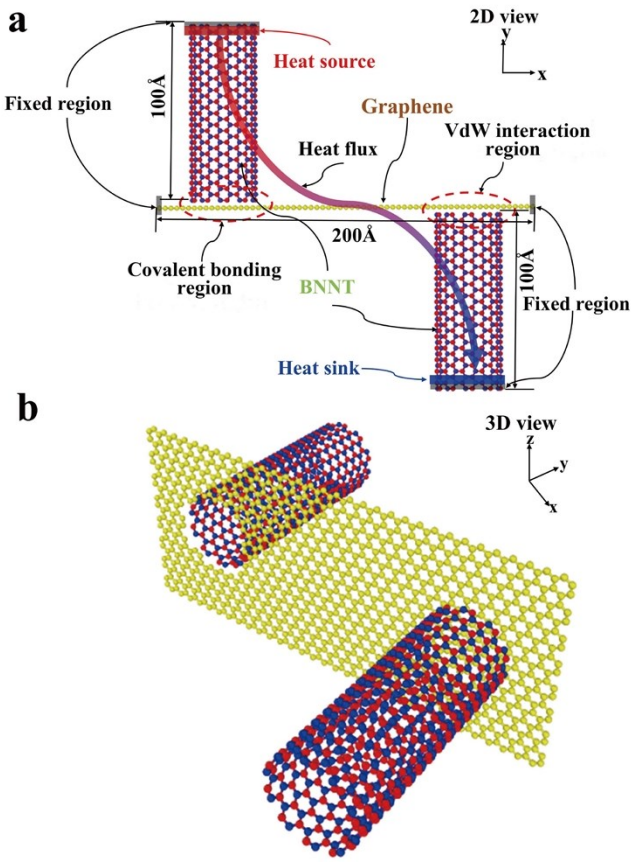

Fig. S14 Molecular model of E-G-BNNT and E-G/BNNT.

The molecular dynamics (MD) simulations in our study were employed using the large-scale atomic/molecular massively parallel simulator (LAMMPS) package as an open-source code. The atomic interaction of boron nitride nanotubes (BNNT) was described using Tersoff potential, and interatomic interaction in the graphene layer was also modeled by Tersoff potential. [1, 2] In addition, the tersoff potential was used to describe the N of the BNNT surface bonded with the C in graphene (covalent C-N bonding). For van der Waal (VdW) interaction, The Lennard-Jones (L-J) 12-6 potential was applied to describe the non-bonded interaction between B, N of BNNT and C of graphene, where $\varepsilon_{C\text{-}B}$ = 5.97 mev, $\sigma_{C\text{-}B}$ = 3.533 Å , $\varepsilon_{C\text{-}N}$ = 3.696 mev and $\sigma_{C\text{-}N}$ = 3.345 Å.[3]

In order to simulate the effect of C-N covalent bonding and no-covalent bonding between BNNT and graphene on the thermal conductivity of the interface, a BNNT-graphene-BNNT model was established. Two 100 Å long BNNT (10_10) were located on the upper and lower sides of the graphene surface, respectively, which the graphene sheet was 40.31 Å*200 Å, and the BNNT was located 20 Å from both ends of the graphene. In addition, the distance between BNNT and graphene sheet was 1.6 Å.

Non-equilibrium molecular dynamics (NEMD) method were performed to study the heat transfer of the covalent bonding and Van der Waals (VdW) between BNNT and graphene layer. A time step of 0.25fs was applied to the integration with the atomic motion of the all simulations. The fixed boundary conditions were applied both in the X and Y direction, and the periodic boundary conditions was

imposed in the Z directions. The fixed regions in the X and Y directions were located at both ends of the system. The adjacent layers next to the fixed regions were grouped as heat source and heat sink, respectively, at both ends of the Y direction of the system. The equilibration stage of system consists of three steps. At first the energy minimization of the system was performed on the optimized positions of the atoms by using the conjugate gradient scheme at 300 K. Once the system energy was minimized, the relaxed system was well equilibrated in the isothermal-isobaric ensemble (i.e., constant number of atoms, temperature and pressure P=0 atom) using a Nosé-Hoover thermostat at 300 K for 0.5 ns for structural relaxations. Finally, the whole system was relaxed in a canonical NVT ensemble (i.e., constant number of atoms, volume and temperature) using a Nose-Hoover thermostat at 300 K for 0.5 ns to reach thermal equilibrium at a designated temperature. When the equilibrium was established, the system was then simulated using a microcanonical NVE ensemble (i.e, constant number of atoms, volume and energy) with a heat source (350K) and heat sink (250K) controlled using Langevin thermostats in the 12 ns of the energy exchange. The typical temperature profile, interfacial thermal conductance and the accumulated thermal energies as a function of the time at the steady state were determined by time averaging 0.5 ns, during the final 6 ns were performed.

The interfacial thermal conductance (G) was then calculated as

$$G = {}^{Q}/_{\Delta T}$$

Where $\triangle$T is the temperature discontinuity/jump at the interface between graphene and BNNT. [4] When steady state was obtained, the heat flux Q can be obtained from the energy transfer rate dE/dt between the source/sink and the thermostats. [5]

$$Q = \frac{dE/dt}{S}$$

where E is the accumulated energy, t is the simulation time in NVE ensemble, and S is the cross-sectional area perpendicular to the transport direction.

Phonon Density of States (PDOS)

The phonon transport across two interface materials can be obtained by the overlap of the PDOS between them. To analyze the mechanism of the interface atoms between BNNT and graphene system, the phonon vibrational density of states (PDOS) can be located via a Fourier transform of the atomic velocity autocorrelation function (VACF) of atoms at the equilibrium state.

$$D(\omega) = \int_0^{\tau} \Gamma(t) cos(\omega t) dt$$

where ω, D(ω), τ and Γ(t) are angular frequency, vibration density of state at frequency ω, the total time and the velocity autocorrelation function of atoms, respectively, and it is given by

$$\Gamma(t) = \langle v(t) v(0) \rangle$$

where v(t) is the atom velocity at time t, $and\ \langle \cdots \rangle$ denotes time and atom number-averaged velocity autocorrelation function. The data related to PDOS were calculated by MATLAB R2018b software.

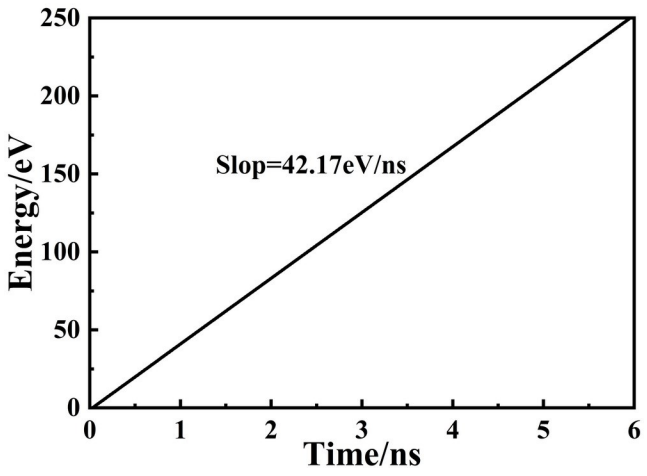

Fig. S15 the accumulated thermal energies (averaged over the heat source and the heat sink) as a function of the time in steady state.

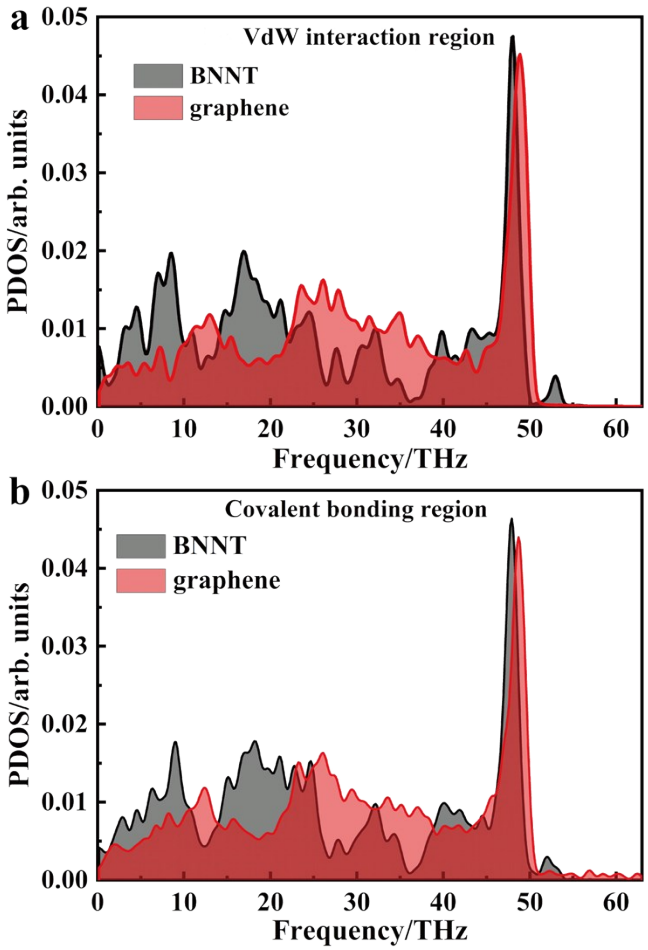

Fig. S16 the phonon density of states (PDOS) for graphene and BNNT of VdW interaction (a) and covalent bonding (b).

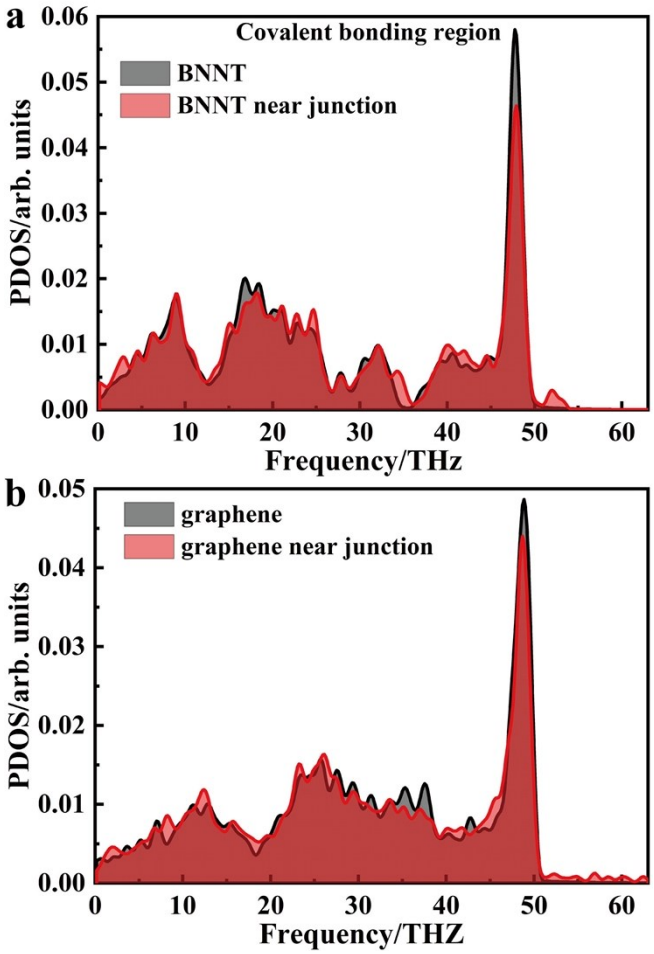

Fig. S17 the PDOS of BNNT (a) and graphene (b) in the E-G-BNNT were compared with those of pure graphene and BNNT.

References

1. L. Lindsay and D. A. Broido, *Phys. Rev. B*, 2010, **81**, 205441.
2. A. Kınacı, J. B. Haskins, C. Sevik and T. Çağın, *Phys. Rev. B*, 2012, **86**, 115410.
3. H. Yang, Z. Zhang, J. Zhang and X. C. Zeng, *Nanoscale*, 2018, **10**, 19092-19099.
4. R. Ma, X. Wan, T. Zhang, N. Yang and T. Luo, *ACS Omega*, 2018, **3**, 12530-12534.
5. H. Dong, Z. Fan, L. Shi, A. Harju and T. Ala-Nissila, *Phys. Rev. B*, 2018, **97**, 094305.